

LIS1 Regulates CNS Lamination by Interacting with mNudE, a Central Component of the Centrosome

Yuanyi Feng,* Eric C. Olson,* P. Todd Stukenberg,^{†||} Lisa A. Flanagan,[‡] Marc W. Kirschner,[†] and Christopher A. Walsh*[§]

*Department of Neurology
Beth Israel Deaconess Medical Center
Harvard Institutes of Medicine
77 Avenue Louis Pasteur

[†]Department of Cell Biology
Harvard Medical School
240 Longwood Avenue

[‡]Department of Medicine
Brigham and Women's Hospital
221 Longwood Avenue
Boston, Massachusetts 02115

Summary

LIS1, a microtubule-associated protein, is required for neuronal migration, but the precise mechanism of LIS1 function is unknown. We identified a LIS1 interacting protein encoded by a mouse homolog of *NUDE*, a nuclear distribution gene in *A. nidulans* and a multicopy suppressor of the *LIS1* homolog, *NUDF*. mNudE is located in the centrosome or microtubule organizing center (MTOC), and interacts with six different centrosomal proteins. Overexpression of mNudE dissociates γ -tubulin from the centrosome and disrupts microtubule organization. Missense mutations that disrupt *LIS1* function block LIS1-mNudE binding. Moreover, misexpression of the LIS1 binding domain of mNudE in *Xenopus* embryos disrupts the architecture and lamination of the CNS. Thus, LIS1-mNudE interactions may regulate neuronal migration through dynamic reorganization of the MTOC.

Introduction

Development of the cerebral cortex depends upon the precise control of neuronal migration. Neurons destined for the cerebral cortex arise from progenitor cells deep in the brain, then migrate long distances to their final destination in a six-layered adult cortex (Rakic, 1978; Gleeson and Walsh, 2000). Lissencephaly (meaning "smooth brain") is a severe genetic brain malformation that causes profound mental retardation, seizures, and other neurological abnormalities (Jellinger and Rett, 1976; Walsh, 1999). The cerebral cortex of the lissencephalic brain is abnormally thick and poorly organized (Kuchelmeister et al., 1993) due to defects in neuronal migration (Alvarez et al., 1986). Heterozygous mutations in the autosomal *LIS1* gene (Reiner et al., 1993) and mutations in the X-linked *DCX* gene (Gleeson

et al., 1998) cause very similar histological patterns of lissencephaly, suggesting that their gene products have related roles (Berg et al., 1998). Moreover, both *LIS1* and *DCX* proteins regulate the microtubule cytoskeleton (Sapir et al., 1997; Francis et al., 1999; Gleeson et al., 1999).

LIS1 encodes a ubiquitously expressed 45 kDa protein with seven WD40 repeats (Reiner et al., 1993) and has recently been shown to be a microtubule-associated phosphoprotein that interacts with tubulin and regulates microtubule dynamics in vitro (Sapir et al., 1997, 1999a). However, studies from several species also suggested roles for *LIS1* not only in migrating cortical neurons, but also in both nuclear translocation and mitosis, suggesting conserved mechanisms of microtubule regulation by the *LIS1* protein. While heterozygous *LIS1* mutant mice show neuronal migration defects analogous to those seen in humans with heterozygous mutations, homozygous null mice show postimplantation lethality, while compound heterozygous *LIS1* mutants show apparent defects in neurogenesis (Hirotsumi et al., 1998), suggesting roles for *LIS1* in neuronal cell division and early development. The yeast protein PAC1 shows 33% sequence identity with *LIS1* and is required for nuclear orientation and mitotic chromosome segregation (Geiser et al., 1997). In the fungus *Aspergillus nidulans*, the *NUDF* protein shares 42% sequence identity with *LIS1* (Xiang et al., 1995) and is essential for nuclear migration, which allows the even distribution of nuclei along the fungal hyphae (Morris et al., 1998b). A *Drosophila* homolog of *LIS1* is required for germline cell division and oocyte differentiation (Liu et al., 1999). The *Drosophila* *Lis1* may also act as a cortical anchor for dynein and maintain membrane integrity during oogenesis (Swan et al., 1999). Given the many potential roles for *LIS1*, the mechanism by which *LIS1* facilitates neuronal migration has remained unclear.

In order to study the mechanism of *LIS1* in neuronal migration, we identified *LIS1* binding proteins using the yeast two-hybrid screen. One *LIS1* binding protein represents a mouse homolog of the nuclear migration gene *RO11* of *N. crassa* (Minke et al., 1999) and the nuclear migration gene *nudE* of *A. nidulans* (Efimov and Morris, 2000). Since *nudE* was identified as a multicopy suppressor of *nudF*, it likely encodes a downstream effector of the *NUDF* protein, suggesting that mammalian mNudE might analogously represent an effector of *LIS1*.

Here we show that mNudE is located at the centrosome and that it acts as a scaffold that binds to multiple centrosomal proteins including γ -tubulin, pericentrin, mitotin, CEP110, TCP-1, SLAP, and the 8 kDa light chain of dynein. Overexpression of mNudE disrupts the normal interphase microtubule network, suggesting that mNudE may normally organize and regulate microtubule structure in migrating neurons. Moreover, disruption of *LIS1*-mNudE interactions is associated with defects in neuronal architecture, since (1) human point mutations associated with lissencephaly disrupt *LIS1*-mNudE binding and (2) overexpression of a dominant negative mNudE construct in *Xenopus* embryos disrupts

[§]To whom correspondence should be addressed (e-mail: cwash@caregroup.harvard.edu).

^{||}Present address: Department of Biochemistry and Molecular Genetics, University of Virginia Medical School, Health Systems Box 800733, Charlottesville, Virginia 22908.

the normal lamination of the anterior CNS. Our data suggest that regulating the structure of microtubule-organizing centers (MTOCs) through LIS1-mNudE interactions is critical to migrating neurons.

Results

Identification of Proteins that Bind to LIS1

We used a yeast two-hybrid screen to identify proteins that interact with LIS1 (Vojtek et al., 1993). Among the clones recovered, 31 encoded a previously identified LIS1 interactor, NudC (Morris et al., 1998a), while 14 encoded a new mouse protein homologous to the MP43, *nudE*, and *RO11* genes. MP43 is a *Xenopus* mitotic phosphoprotein (Stukenberg et al., 1997), while *nudE* and *RO11* are required for nuclear migration in the fungi *A. nidulans* and *Neurospora crassa*, respectively (Minke et al., 1999; Efimov and Morris, 2000). Notably, *nudE* is a multicopy suppressor of *nudF*, the *A. nidulans* homolog of *LIS1* (Efimov and Morris, 2000), suggesting that NUDE protein functions as a downstream effector of NUDE. Therefore, the murine homolog of the NUDE protein, which we refer as mNudE, may be downstream of LIS1.

The full-length cDNA of mNudE encodes a 344 amino acid protein with a predicted molecular weight of 40 kDa (Figure 1). mNudE shares 64% sequence identity (74% similarity) with MP43 over the entire length of both proteins. In addition, mNudE shows 33% sequence identity (46% similarity) to NUDE and 35% identity (50% similarity) to RO11 (data not shown), though both fungal genes encode an extended C terminus that is not present in mNudE. The mouse mNudE is 86% identical to rNUDE from rat (Kitagawa et al., 2000), while a human EST (GenBank Accession #BAA90949 and labeled as hNudE in Figure 1) and a related *Drosophila* gene CG8104 (GenBank Accession #AAF50184) encode proteins with 87% and 32% sequence identity (90% and 50% similarity) with the mouse protein, respectively (Figure 1A). Thus, like *LIS1*, *NUDE* is highly conserved evolutionarily. Another LIS1-interacting protein, Nudel, identified recently (Sasaki et al., 2000 [this issue of *Neuron*]; Niethammer et al., 2000 [this issue of *Neuron*]) also shows high sequence homology with the NUDE protein. The mouse *mNudE* and *Nudel* encode proteins of similar size that are 55% identical in full-length sequence and 85% identical in the LIS1 binding domain (Figure 1D).

Although mNudE lacks distinctive structural motifs, its predicted structure suggested an amino-terminal coiled-coil stretch (Figure 1B) that is the most highly conserved segment of the protein evolutionarily (Figure 1A). Moreover, this region of NUDE by itself is sufficient to complement the *nudE* deletion and suppress the *nudF* mutation in *Aspergillus*, indicating that the coiled-coil domain is sufficient for NUDE's function (Efimov and Morris, 2000). Analyses of phosphorylation motifs (Songyang and Cantley, 1998) showed that mNudE is a potential substrate for many protein kinases (Figure 1C), suggesting that mNudE is regulated by phosphorylation. Moreover, MP43, the *Xenopus* homolog of mNudE, was isolated as a protein specifically phosphorylated in mitosis (Stukenberg et al., 1997), so that mNudE may resemble MP43 in being a target of cell cycle-dependent kinases.

LIS1 Binds mNudE Specifically

In order to investigate the specificity of LIS1-mNudE binding, we performed coimmunoprecipitation and GST pulldown experiments. mNudE was myc tagged, expressed in 293T cells, and immunoprecipitated with anti-myc antibody from whole-cell extracts. Immunoprecipitates were analyzed for the presence of LIS1 by immunoblotting. To avoid interference between LIS1 (45 kDa) and the IgG (the 50 kDa heavy chain) used in the immunoprecipitation, immunoprecipitates were separated by nonreducing SDS-PAGE, on which LIS1 appears as several bands (Morris et al., 1998a). LIS1 specifically coimmunoprecipitates with myc-mNudE (Figure 2A), indicating that myc-mNudE associated with LIS1 when expressed in 293T cells. Native LIS1 protein from E16 and P1 mouse brain homogenates also binds to mNudE immobilized on glutathione sepharose beads as a GST fusion protein (Figure 2B).

The 14 mNudE clones recovered in our two-hybrid screen allowed us to define the LIS1-interacting region of mNudE. Clones 13 and 87 encode amino acids 20–159 and 90–272 of mNudE, respectively, suggesting that the LIS1 binding domain lies between amino acids 90–159. This region is part of the predicted coiled-coil structure, a motif that can mediate protein-protein interactions. A GST fusion protein containing amino acids 88–156 of mNudE (GST-DN) efficiently bound LIS1 from brain homogenates (Figure 2B), suggesting that the LIS1 binding domain lies between amino acids 90 and 156.

Lissencephaly-Causing *LIS1* Mutations Abrogate mNudE Binding

To test the importance of LIS1-mNudE interactions for LIS1 function, we examined whether missense mutations in *LIS1* that cause human lissencephaly (Lo Nigro et al., 1997; Pilz et al., 1999) disrupt LIS1-mNudE binding. Point mutations H149R and S169P were constructed in the LIS1 cDNA and then either fused to LexA or myc tagged. Both of the *LIS1* missense mutations completely abolish LIS1-mNudE interaction in the two-hybrid assay (Figure 2C). Furthermore, the two mutated LIS1 proteins failed to bind mNudE by coimmunoprecipitation (Figure 2D). Although others have claimed that the H149R and other *LIS1* mutations are unstable (Sapir et al., 1999b), in our hands, the LIS1 missense mutations were expressed at levels comparable to the wild-type protein (Figure 2D). Moreover, COS-7 cells transfected with the myc-tagged LIS1 mutant constructs expressed the mutant constructs with distributions indistinguishable from wild-type myc-LIS1 (data not shown). Our data therefore suggest that the interaction of LIS1 with mNudE is specific and may be essential for LIS1's function in neuronal migration.

mNudE Is a Developmentally Regulated, Ubiquitously Expressed Protein

The mNudE mRNA is expressed widely in the developing brain. Northern hybridization using two probes containing nucleotide sequences 1–1021 and 728–1545 of the mNudE cDNA revealed a major mRNA species of ~2.5 kb and a minor band at ~4 kb in mouse embryos (Figure 3A). The mNudE mRNA level peaks around embryonic day 11 (E11) and decreases at E15 and E17.

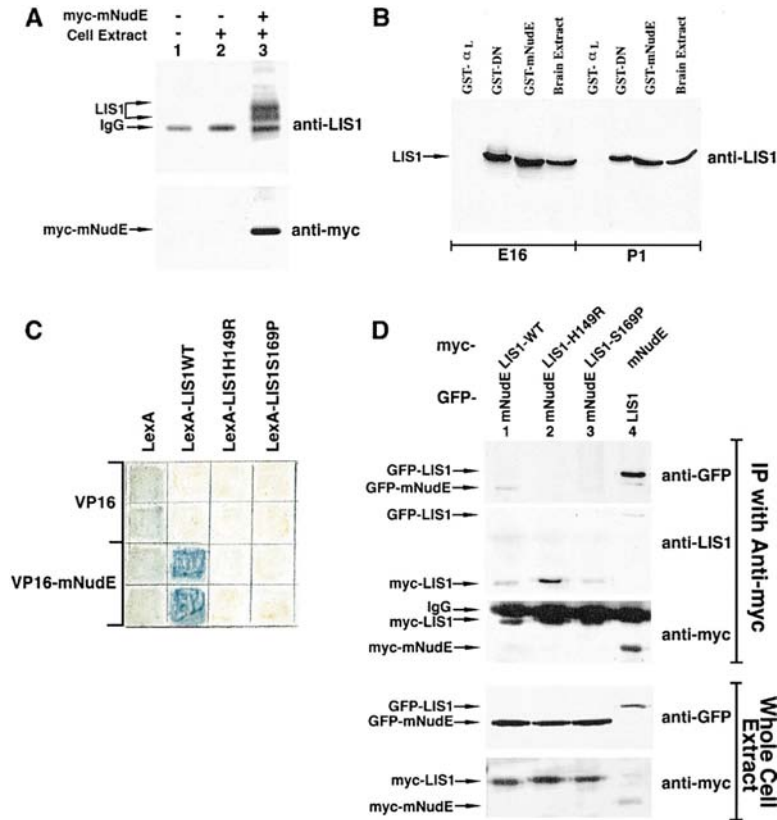


Figure 2. LIS1-mNudE Interaction

(A) Coimmunoprecipitation of LIS1 with mNudE. Myc-mNudE in pcDNA3 vector or vector alone were transfected in 293T cells, and cells were harvested 44 hr after transfection. Whole-cell protein extracts were made in lysis buffer I (see Experimental Procedures), and immunoprecipitations were performed using 2 μ g anti-myc monoclonal antibody 9E10. The immunoprecipitates were dissolved with nonreducing SDS sample buffer, analyzed by SDS-PAGE, followed by immunoblotting with a monoclonal antibody to LIS1 (note that LIS1 shows more than a single band under nonreducing condition), or anti-myc 9E10, as indicated. Immunoprecipitation from empty vector transfected 293T cell protein extracts (myc-mNudE -) or lysis buffer (Cell Extract -) served as negative controls. (B) Binding of LIS1 to GST-mNudE. GST fusion proteins of full-length mNudE (GST-mNudE), mNudE amino acids 88–156 (GST-DN), and the cytoplasmic domain of Integrin α subunit (GST- α L) were expressed in bacteria strain BL21 and purified on glutathione sepharose. Purified GST proteins were incubated with protein extracts from E16 or P1 mouse brain in lysis buffer I. After washing off unbound proteins, proteins bound to the GST beads were analyzed by standard SDS-PAGE followed by immunoblotting with a monoclonal anti-LIS1 antibody. (C) Two-hybrid interaction of mNudE with wild-type LIS1 and LIS1 mutant proteins corresponding to previously identified lissencephaly mutations.

The interaction of mNudE with LIS1, LIS1-H149R, and LIS1-S169P were examined by the two-hybrid filter assay. mNudE was fused to the VP16 transactivation domain. LIS1, LIS1-H149R, and LIS1-S169P were fused to LexA. VP16 and LexA fusion plasmids were cotransformed into L40 strain. Two individual transformants were patched and assayed on filter paper as described in the Experimental Procedures. The activity of interaction is indicated by the blue β -galactosidase product.

(D) Coimmunoprecipitation of mNudE with wild-type LIS1 and mutant LIS1 proteins. LIS1 and mNudE were tagged with GFP and the c-myc 9E10 epitope, respectively. LIS1-H149R, and LIS1-S169P were tagged by the c-myc 9E10 epitope. LIS1 and mNudE constructs were cotransfected into 293T cells. Whole-cell protein extracts (Whole-cell Extract) were made in lysis buffer I 44 hr after transfection, and immunoprecipitation was performed with the 9E10 monoclonal antibody, which directly immunoprecipitates myc-tagged LIS1 proteins (lanes 1–3) and myc-mNudE (lane 4). Immunoprecipitates and whole-cell protein extracts were analyzed by SDS-PAGE followed by immunoblotting with indicated antibodies. As indicated on the polyclonal anti-GFP immunoblot, GFP-LIS1 and GFP-mNudE coimmunoprecipitate with myc-mNudE and myc-LIS1, respectively. However, GFP-mNudE signal was not detected in the immunoprecipitates of LIS1 mutants, although these mutants appeared to be expressed and present in the immunoprecipitates at a similar level to the wild-type LIS1 as indicated by both LIS1 and 9E10 antibody blots.

Like LIS1, mNudE is expressed in all tissues examined (Figure 3B), with relatively higher expression in kidney and spleen. Expression of mNudE in brain is higher at early embryonic stages and lower during late embryogenesis (Figure 3C). In situ hybridization at E14 showed that mNudE is highly expressed in the ventricular zone and the intermediate zone of the cerebral cortex (Figures 3D and 3E). Although mNudE is downregulated at E15.5, it was still detectable in the ventricular zone, intermediate zone, and at lower levels in cortical plate (Figure 3F).

Expression of mNudE in developing cerebral cortex was confirmed by immunohistochemical analyses. A polyclonal anti-peptide antibody for mNudE produced immunoreactivity in the E16 ventricular zone, intermediate zone, and in the cortical plate neurons (Figures 3G and 3H). These data suggest that mNudE is present in proliferating neuronal progenitors as well as migrating neurons.

The LIS1 Binding Domain of mNudE Induces Anterior Neuronal Defects in *Xenopus* Embryos

In order to test whether LIS1-mNudE interactions are required for neuronal migration, we took a dominant-

negative approach in *Xenopus* embryos to specifically disrupt LIS1-mNudE/MP43 interactions. If interactions between mNudE/MP43 and LIS1 mediate LIS1's role, then misexpression of just the LIS1-interacting domain of mNudE should competitively block normal LIS1-mNudE interaction and disrupt neuronal migration. The *Xenopus* NUDE homolog, MP43, is strongly expressed in the eye, branchial arches, and telencephalon (Figures 4A and 4B, arrows) in Nieuwkoop and Faber (N&F) stage 26–33 albino embryos. In the early neurula (N&F stage 13), little or no message was detected in the neural plate, with the possible exception of the dorsal lip of the closing blastopore (data not shown). The timing and extent of the expression is consistent with MP43 playing a selective role in later neurogenesis in *Xenopus*.

To interfere with normal LIS1-MP43 interactions, a truncated mNudE construct was created, which took the advantage of the fact that mNudE 88–156 (mNudE-DN) binds to LIS1 as efficiently as the full-length mNudE (Figure 2B) and that the amino acid sequence of this LIS1 binding region is 90% identical (93% similar) between *Xenopus* and mouse (Figure 1A). An mRNA encoding

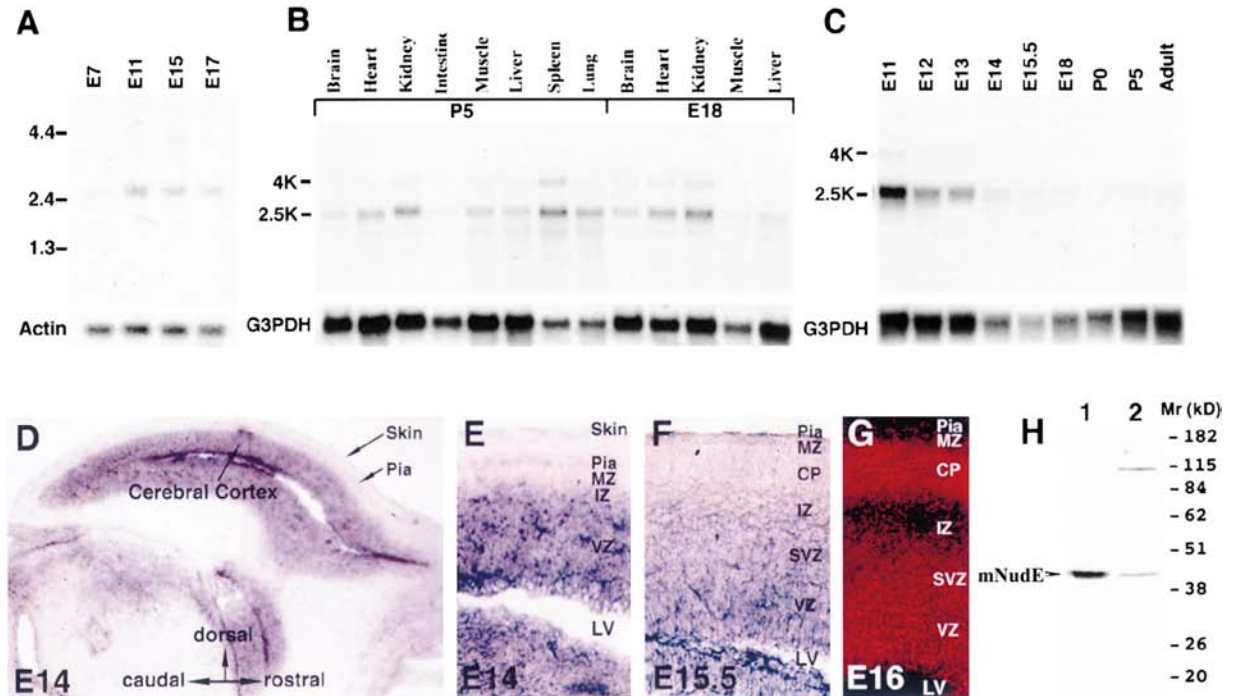


Figure 3. mNudE Expression Analyses

(A) Northern blotting analysis of mNudE expression with Poly-A RNA from mouse whole embryos. A mouse whole embryo Poly-A RNA blot was purchased from Clontech and normalized with a β -actin probe. mNudE mRNA was examined by hybridizing the blot with a mNudE cDNA fragment encoding nucleotides 1–1021. A major message at \sim 2.5kb was observed, and a weak band at \sim 4 kb was also detected.

(B) The expression of mNudE mRNA from various mouse tissues. Total RNAs were extracted from embryonic day 18 (E18) and postnatal day 5 (P5) mouse, 5 μ g RNA was loaded into each lane, and the blot was probed with a mNudE probe representing nucleotides 1–1021. A mouse G3PDH probe was used as a loading control. The same blot was probed with another mNudE probe representing nucleotides 718–1545 and showed similar results (data not shown).

(C) Northern blot analysis shows that mNudE mRNA in mouse brain is developmentally regulated. Mouse brain total RNAs from embryonic day 11 (E11) to adult were extracted and analyzed on Northern blots. 10 μ g total RNA was loaded into each lane, and the blot was probed with a mNudE cDNA fragment representing nucleotides 718–1545, then stripped, and re-probed with a G3PDH control probe. The same blot was probed with another mNudE probe representing nucleotides 1–1021 and showed similar distribution (data not shown).

(D–F) mNudE is expressed in the mouse cerebral cortex. In situ hybridization with a mNudE probe shows that mNudE mRNA is highly expressed in E14 mouse cerebral cortex. Strong expression was detected at the ventricular zone of the cortex (sagittal sections, [D and E]). At E15.5, weak, specific signals were detected in the ventricular zone, subventricular zone, intermediate zone, and cortical plate (coronal section, [F]). Two independent mNudE probes showed consistent distribution, and a sense strand probe showed no hybridization signal (data not shown).

(G) Immunohistochemical staining of mNudE in mouse E16 cerebral cortex. A mouse E16 brain was cryosectioned, fixed with -20°C methanol, and stained with mNudE anti-sera. mNudE immunoreactivity was detected by a Cy3-conjugated goat anti-rabbit antibody in cortical plate, intermediate zone, and ventricular zone. MZ, marginal zone; CP, cortical plate; IZ, intermediate zone; SVZ, subventricular zone; VZ, ventricular zone; LV, lateral ventricle.

(H) Immunoblotting with mNudE anti-sera showing the presence of a 40 kDa protein in embryonic mouse brain. Protein extracts from mouse E12 brain were made in a detergent-free buffer (see Experimental Procedures) and analyzed on an immunoblot probed with affinity purified mNudE antisera. The antisera detected the recombinant mNudE protein expressed in COS-7 cells (lane1) and a protein of same size from E12 mouse brain (lane2). The slow-migrating band from the E12 brain sample may represent a SDS insoluble complex of mNudE since the intensity of this band increases with sample storage time.

amino acids 88–156 of mNudE was injected into prospective right blastomeres of *Xenopus* embryos at the two- to four-cell stage, and injected embryos were analyzed at stage 40 or later. Injection into one cell of a two-cell embryo allows RNA expression in only one half of the embryo, leaving the other half of the embryo undisturbed, acting as an internal control. Embryos (N&F stage 46) injected with the GFP RNA appeared normal (Figure 4C), as did embryos injected with 1ng/blastomere of full-length mNudE mRNA (data not shown). Higher levels of mNudE mRNA (\geq 2 ng/blastomere) produced many teratogenized embryos, which were not analyzed further. In contrast to GFP and full-length mNudE mRNA injections, embryos injected with mNudE-

DN mRNA showed smaller anterior structures and deformed and smaller eyes on the injected side (Figures 4D and 4E, arrows). The rest of the body was grossly normal. The small eye phenotype observed in the mNudE-DN misexpressing embryos was highly penetrant, so that 50% of the embryos that received mNudE-DN showed grossly reduced eyes on the injected side (Table 1).

To clarify the phenotype of mNudE-DN misexpression, stage 40 embryos were analyzed histologically. The uninjected side of the embryo showed normal eye morphology (Figures 4F and 4G). On the side (right) that received mNudE-DN injection, sections through the eye showed a spectrum of retinal phenotypes. Mildly af-

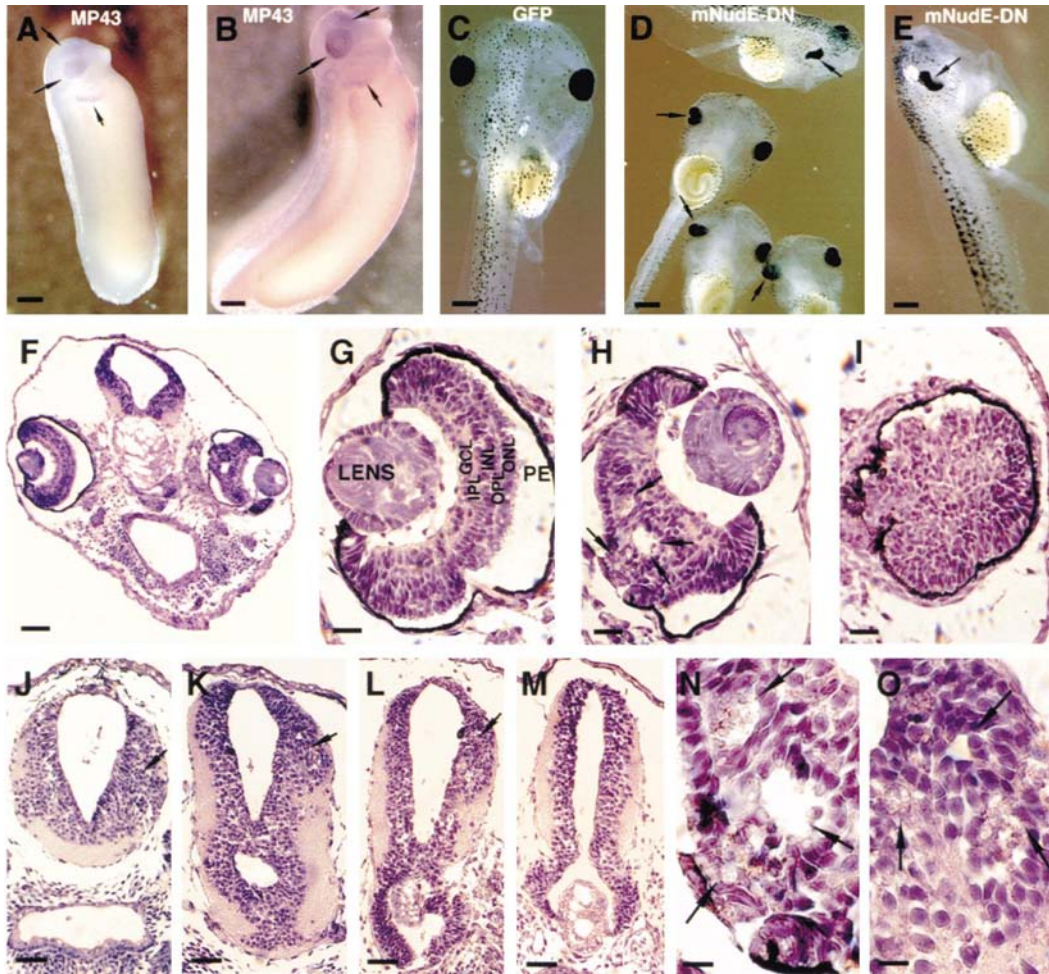


Figure 4. Blocking of LIS1-mNudE Interactions Disrupts CNS Lamination

(A and B) In situ hybridization for MP43 mRNA in *Xenopus* embryos. The expression of the mNudE *Xenopus* homolog MP43 was examined by whole-mount in situ hybridization with albino *Xenopus* embryos using a MP43 probe. (A) and (B) show the distribution of MP43 mRNA in two representative embryos at stage 26 and 33. Strong signals were observed in the eye, branchial arches, and the telencephalon (arrows). Scale bars: 400 μm .

(C–E) Blocking LIS1-MP43 interactions by mNudE-DN causes abnormal eye development in *Xenopus*. mRNAs were injected to *Xenopus* embryos at the two-cell or four-cell stage, and the embryos were allowed to develop to stage 40 and later. A representative embryo (N&F stage 46) injected with GFP mRNA shows normal morphology (C). In contrast, same stage embryos that received mNudE-DN injection show deformed and reduced eyes on the injected (right) side as indicated by arrows (D and E). Scale bars: (C and E), 200 μm ; (D), 325 μm .

(F–O) Histological analysis of the eye and brain defects caused by mNudE-DN misexpression. Stage 40 embryos were fixed, embedded in paraffin, sectioned at 5 μm , and stained with haematoxylin and eosin (H&E). Sectioning through the embryos that received mNudE-DN mRNA injection show that the left (uninjected) side has normal eye morphology and retina lamination as indicated in (F) and (G) (ONL, outer nuclear layer; OPL, outer plexiform layer; INL, inner nuclear layer; IPL, inner plexiform layer; GCL, ganglion cell layer; PE, pigmented epithelium). On the right side that received mNudE-DN, the retinas show focal thickening and disorganization (F and H) as indicated by arrows (H). Ectopic photoreceptor cones are found deep to the surrounding aberrant cell sparse cavities (H and N). In the more severely affected eyes, the lens is missing and the retina exhibits little discernible lamination (I). The nonneural tissues surrounding the affected eye do not appear abnormal (F). Brain sections reveal dysplasia and suggest abnormal lamination on the mNudE-DN injected side (arrows). Along the rostral caudal axis, cellular layers of the telencephalon appears thicker (J–L), and the projection of optic tract into the tectum is disorganized (K, L, and O). Cell sparse cavities are occasionally observed in the brain on the injected side (K and O). A representative embryo that received GFP mRNA injection has normal symmetrical structure of cellular layers and optical fiber tracks (M).

Scale bars: (F), 100 μm ; (G–I), 33 μm ; (J–M), 50 μm ; (N and O), 12.5 μm .

affected eyes were 10%–20% smaller along the dorsal-ventral axis, with focal thickening and poor lamination of the retina. In these mildly affected eyes, the photoreceptor-containing outer nuclear layer (ONL), identifiable by the oil droplet-containing photoreceptor cone cells, was often interrupted by dysplastic tissue. Similarly the fibers of the retinal ganglion cells layer (GCL) were disor-

ganized, and the inner and outer plexiform layers (IPL, OPL) were disrupted (Figures 4F and 4H, arrows). In more severely affected eyes, the overall dimensions were further reduced, the lens was absent, and the retina exhibited little or no discernible lamination (Figure 4I).

In addition to altering the size and lamination of the retina, mNudE-DN injection also produced abnormal ar-

Table 1. Phenotypes Observed after mNudE-DN mRNA Injection in *Xenopus* Embryos

Construct (Amount Injected)	n	Grossly Abnormal n (%)	Small Eye n (%)		Normal n (%)
			Right Side	Left Side	
GFP (3 ng)	27	0	0	0	27 (100%)
mNudE-DN (1 ng)	78	17 (22%)	39 (50%)	4 (5%)	18 (23%)

chitecture of the cell and fiber layers in the forebrain and midbrain on the injected side. In the rostral telencephalon, neuronal tissue on the injected side was thick and disorganized (Figures 4J and 4K, arrows). Although the forebrain of *Xenopus* does not show the same precise laminar structure that characterizes the cerebral cortex of mammals, the thickened, disordered neuronal architecture is reminiscent of the architectural defects seen in lissencephaly. The tectal midbrain also was thick and disorganized, which is further indicated by the aberrant optic tract projections into the tectum on the right

(mNudE-DN injected) side, but not on the left (uninjected) side (Figures 4K and 4L, arrows). No abnormalities were seen in GFP control injections (Figure 4M). At stage 40, the tectum receives input entirely from the contralateral eye so that the fibers of the tract projecting into the tectum on the injected side are coming from the uninjected side of the embryo. Therefore, the disorganization is apparently due to abnormalities intrinsic to tectum rather than in the fiber tract itself.

In contrast to the severe and consistent CNS malformation, nonneural tissues surrounding the affected eye

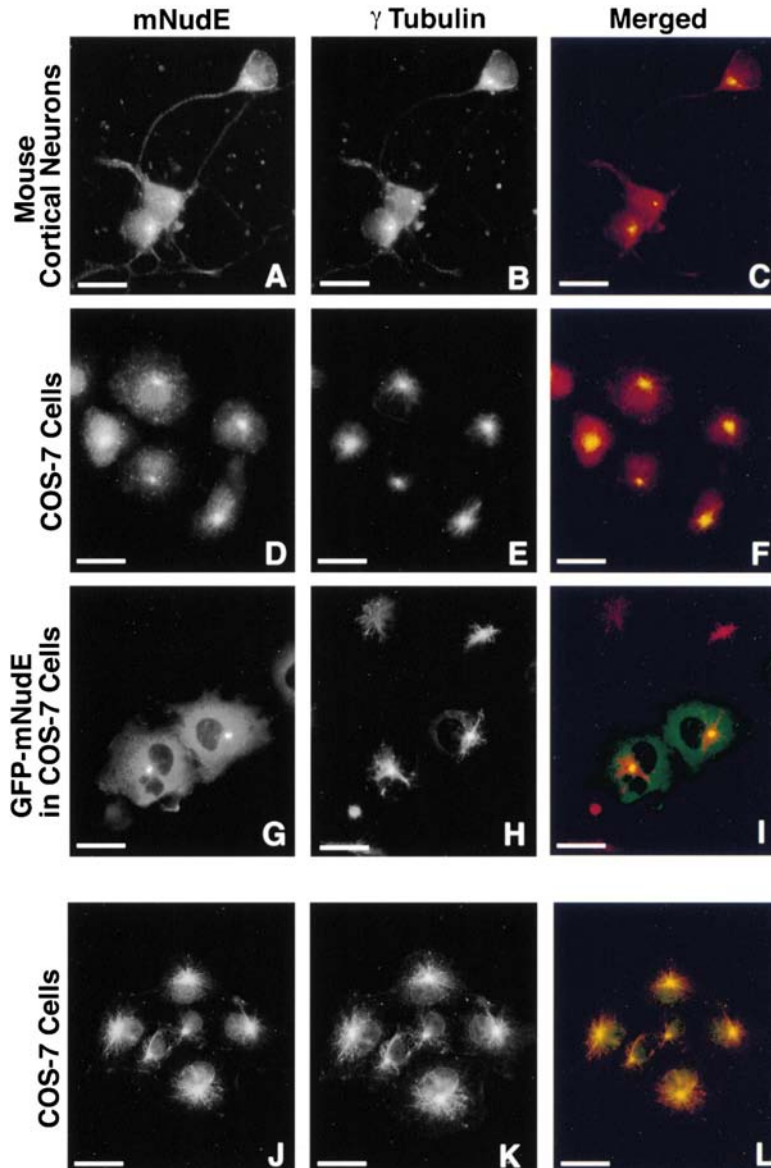


Figure 5. mNudE Is Localized to the Centrosome or MTOC in Neurons and Interphase COS-7 Cells

Mouse cortical neurons were isolated from E16 mouse cerebral cortex and grown on poly-D-lysine coated coverslips in culture for 2 days (A–C). COS-7 cells were grown on coverslips to ~50% confluency (D–L). Cells were fixed with -20°C MeOH, and immunostaining was performed as described (see Experimental Procedures). Cells were double stained with affinity purified mNudE antisera ([A and D], red) and a γ -tubulin monoclonal antibody that serves as the centrosomal marker ([B and E], green). Cells transfected with GFP-mNudE ([G], green) were stained with γ -tubulin monoclonal antibody ([H], red). COS-7 cells were also double stained with the mNudE anti-sera ([J], green) and a polyclonal LIS1 antibody (N-19, Santa cruz, [K], red) to reveal the mNudE-LIS1 colocalization. Individual stainings were shown in gray scale. Red and green staining patterns were merged in Adobe Photoshop, showed in color and labeled as “Merged” images (C, F, I, and L). Scale bars: (A–C), 10 μm ; (D–L), 40 μm .

and brain structures appear normal (Figure 4F), suggesting that neuronal tissue is particularly sensitive to interference of LIS1-mNudE/MP43 interactions, and/or that the abnormalities are limited to areas that express the highest level of MP43. These results suggest that LIS1-mNudE/MP43 interactions have an important role in the migration and/or lamination of central nervous system tissue.

mNudE Is Located in the MTOC and Interacts with Many Centrosomal Proteins

To understand the mechanism of the LIS1-mNudE interactions, we studied the cellular role of the mNudE protein. In COS-7 cells and cultured cortical neurons, mNudE immunoreactivity predominantly concentrated in a distinct perinuclear spot in interphase cells, which is a typical staining pattern for proteins localized at the centrosome or MTOC. Double labeling of mouse cortical neurons and COS-7 cells with mNudE antisera and a centrosomal marker (a monoclonal antibody to γ -tubulin) showed that mNudE and γ -tubulin are colocalized, indicating that mNudE resides in the centrosome (Figures 5A–5F). To further confirm the centrosomal location of mNudE, we expressed a GFP fusion protein of mNudE in COS-7. When cells express GFP-mNudE at low levels, the GFP fluorescence was exclusively localized in the centrosome (Figures 5G–5I), suggesting that the native protein is part of the centrosomal complex. Immunostaining also demonstrated that LIS1 is concentrated at the centrosome of interphase cells and costained with mNudE (Figures 5J–5L). This is consistent with a recent reported by Smith et al. (2000) and suggests that LIS1-mNudE interactions occur at the centrosome.

We further examined possible physical interactions between mNudE, LIS1, and γ -tubulin by transfecting 293T cells with GFP-tagged mNudE or GFP-tagged LIS1. Immunoprecipitation was performed with a γ -tubulin monoclonal antibody and analyzed by nonreducing SDS-PAGE to avoid the interference of IgG with γ -tubulin signals (48 kDa) on the immunoblot. The γ -tubulin antibody selectively brought down full-length GFP-mNudE, or mNudE-GFP, but not GFP-LIS1 or the GFP-mNudE-DN (Figure 6A). This suggests that mNudE forms a complex with γ -tubulin in vivo and that LIS1 may be recruited to the centrosome via an interaction with mNudE, rather than associating with the γ -tubulin complex directly.

Using a yeast two-hybrid screen, we found that many mNudE binding proteins represent known centrosomal components. Among 18 different mNudE-interacting clones, pericentrin, mitotin/CENP-F, TCP-1, CEP110, and SLAP have been shown to be associated with centrosomes (Rattner et al., 1993; Doxsey et al., 1994; Li et al., 1995; Brown et al., 1996; Dichtenberg et al., 1998; Guzzo et al., 1999; Guasch et al., 2000). Another mNudE-interacting clone encoded the 8 kDa light chain (LC8) of cytoplasmic dynein, which is important for dynein motor function and early embryogenesis in *Drosophila* (Dick et al., 1996); its homolog (*NUDG*) in *A. nidulans* is also required for nuclear migration (Xiang, et al., 1999). The dynein light intermediate chain directly interacts with pericentrin and contributes to mitotic spindle organization (Purohit et al., 1999), and there is evidence that cytoplasmic dynein associates with LIS1 and regulates mitosis and microtubule organization (Faulkner et al.,

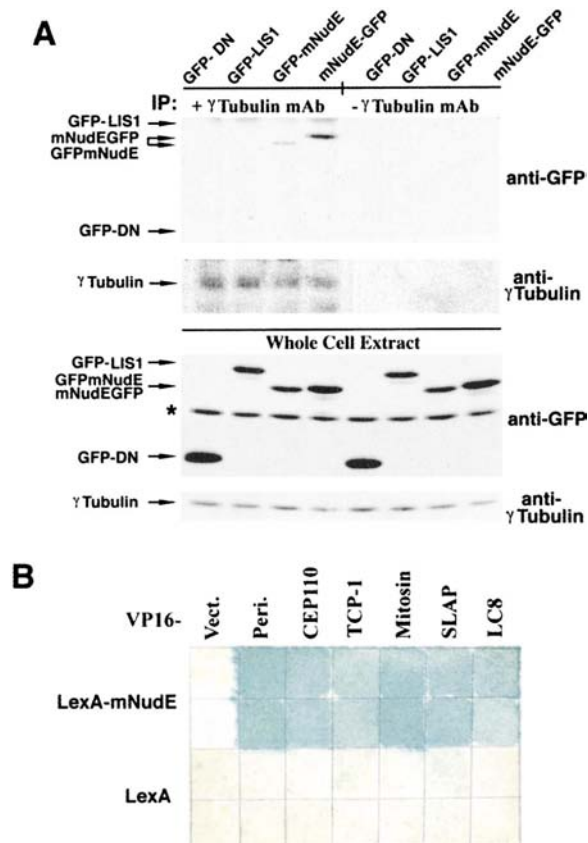


Figure 6. mNudE Is a Central Scaffold of the MTOC

(A) γ -tubulin coimmunoprecipitates with mNudE but not LIS1. GFP-tagged full-length LIS1 (GFP-LIS1), mNudE (GFP-mNudE or mNudE-GFP), and the LIS1 binding domain of mNudE (GFP-DN) were transfected in 293T cells, and whole-cell extracts were made 44 hr after transfection in lysis buffer II (see Experimental Procedures). Immunoprecipitation was performed with a monoclonal anti- γ -tubulin antibody. Immunoprecipitation with mouse IgG or without the addition of antibody were performed in parallel to serve as negative controls. The immunoprecipitates were dissolved in SDS sample buffer in the absence of reducing reagents and analyzed by immunoblotting with a monoclonal anti-GFP antibody (Clontech). Both amino- and carboxyl-GFP-tagged mNudE (GFP-mNudE and mNudE-GFP) coprecipitate with γ -tubulin, whereas GFP-LIS1 and GFP-DN were both absent in γ -tubulin immunoprecipitates. (Note that the N-terminal and C-terminal tagged mNudE run at different positions on a SDS gel under nonreducing condition, although they appear to be the same size under reducing condition). The asterisk denotes a \sim 50 kDa 293T cell protein that cross-reacts with the anti-GFP antibody. (B) Two-hybrid interactions of mNudE with multiple centrosomal proteins. In a two-hybrid screen using the LexA-mNudE as the bait, clones encode partial or full-length sequence of pericentrin (Peri.), mitotin, CEP110, TCP-1, SLAP, and the 8 kDa light chain of cytoplasmic dynein (LC8) were identified. Plasmids from the two-hybrid positive clones were recovered and used to retransform L40 strain with LexA-mNudE or LexA alone. Two individual transformants were patched and assayed on a filter papers. Positive interactions are indicated by the blue β -galactosidase product.

2000; Smith et al., 2000). Therefore, the mNudE-dynein association may also be involved in regulating centrosome or mitotic spindle function.

Overexpressing mNudE Causes Ectopic Nucleation of Microtubules in COS-7 Cells

Since the interaction of mNudE with six different centrosomal proteins suggests that mNudE is a central

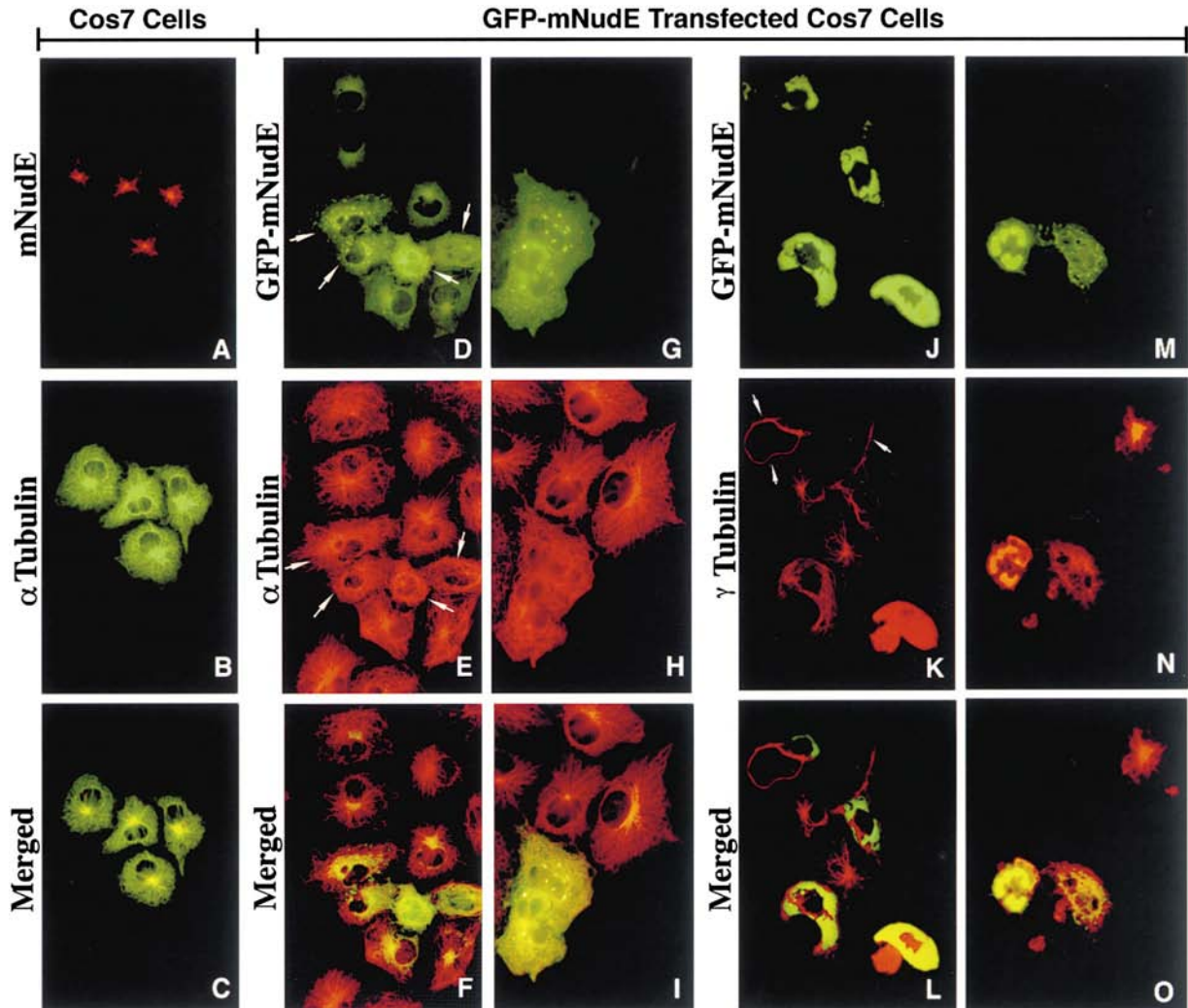


Figure 7. mNudE Overexpression Causes Ectopic Nucleation of Microtubules and Dislocation of γ -Tubulin from Centrosome in COS-7 Cells
 COS-7 cells were grown on coverslip and fixed with -20°C MeOH 28–36 hr after transfection. Immunofluorescence staining was performed as described (see Experimental Procedures). Double staining was performed on untransfected COS-7 cells with mNudE antisera ([A], red) and with monoclonal anti α -tubulin antibody ([B], green). Cells transfected with GFP-mNudE were revealed by the GFP green fluorescence ([D, G, J, and M], green), stained with α -tubulin antibody to reveal the microtubule structure ([E and H], red), and stained with monoclonal anti- γ -tubulin antibody to reveal the distribution of γ -tubulin ([K and N], red). Red and green staining patterns were merged using Adobe Photoshop and labeled as “Merged” images (C, F, I, L, and O). Two fields of GFP-mNudE transfected cells are shown to better represent the spectrum of overexpression phenotypes. In (D) and (E), arrows indicate that cells express the highest level of mNudE show more severe disruption of the centrosome-based radial microtubule network; and in (K), arrows indicate that overexpression of mNudE induce the formation of γ -tubulin fibers.

component of the centrosome, we examined the effects of overexpressing mNudE on the microtubule network. In most interphase mammalian cells, microtubules appear as a highly ordered radial array of tubulin fibers, while γ -tubulin concentrates at the centrosome. In contrast to cells with no or low GFP-mNudE expression, cells that expressed high levels of GFP-mNudE showed profound disruption of the normal centrosome-based, interphase microtubule network (Figures 7A–7I). In these cells, the disordered microtubules appeared to radiate instead from the area of highest GFP-mNudE expression.

Cells that expressed high levels of GFP-mNudE also showed disruption of the normal distribution of γ -tubulin. Immunostaining showed that γ -tubulin was dislocated from the centrosome and lost its normal aster-

shaped staining pattern at the centrosome, showing instead a disorganized or diffuse pattern in the cytoplasm (Figures 7J–7O). In many cells, γ -tubulin was localized in patches corresponding to aggregates of GFP-mNudE protein. In some cases, γ -tubulin cables were also observed (Figure 7K, arrows), which resemble the γ -tubules seen in cells that overexpress γ -tubulin (Shu and Joshi, 1995). As judged by the intensity of the γ -tubulin signal, it appeared that mNudE not only altered the distribution of centrosome-associated γ -tubulin, but also upregulated and recruited soluble γ -tubulin to its vicinity. The observation that mNudE interacts with γ -tubulin and controls its distribution suggests that mNudE regulates the formation of the MTOC and hence determines the organization of the microtubule network.

Discussion

In this study, we identified a LIS1-interacting protein, mNudE, and showed that mNudE is likely to be a downstream effector of LIS1. mNudE is a developmentally regulated, widely expressed protein and is localized in the centrosome of interphase cells including cortical neurons. It associates with multiple centrosomal proteins, and overexpression of mNudE alters γ -tubulin distribution and microtubule organization in interphase cells. LIS1 missense mutations that produce stable proteins incapable of supporting neuronal migration also disrupt binding to mNudE. Moreover, blocking LIS1-mNudE/MP43 interactions produces cytoarchitectural defects in the retina, forebrain, and tectum of *Xenopus* embryos. Our results suggest that mNudE is a critical link through which LIS1 regulates the structure and dynamics of microtubules in neurons and suggest that LIS1-mNudE interactions play essential roles in the generation of normal CNS laminar architecture.

mNudE Is a Central Component of the Centrosome

Our data suggest that mNudE is a central component of the centrosome and potentially other MTOCs and that mNudE plays a pivotal role in MTOC function and therefore in microtubule organization. Although microtubules are simple homogenous polymers of α - and β -tubulin, they can form diverse structural arrays with distinct functions. In eukaryotic cells, the de novo synthesis of microtubules is initiated and regulated by MTOCs. The centrosome is the major MTOC in eukaryotic cells and provides microtubule nucleation sites and directs microtubule polymerization so that the minus ends of the microtubules are in contact with the centrosome. Interactions of mNudE with multiple centrosomal proteins imply that mNudE may represent a scaffold that organizes MTOCs. Consistent with a possible scaffold role of mNudE, we find that overexpression of mNudE in COS-7 cells causes formation of ectopic MTOCs. Although the mechanism of microtubule nucleation at the centrosome is not yet clear, γ -tubulin is essential, possibly by interacting directly with α , β -tubulin heterodimers similar to the interactions between heterodimers during microtubule elongation (Stearns et al., 1991; Stearns and Kirschner, 1994). In vertebrate somatic cells, 80% of the γ -tubulin is present in the cytoplasm in a large ring like complex (γ -TuRC; Zheng et al., 1995). The recruitment of this soluble γ -tubulin is essential for the formation of functional MTOCs and initiation of microtubule polymerization. The physical association of mNudE with γ -tubulin and the alteration of the localization and organization of γ -tubulin by overexpressed mNudE suggest that mNudE can directly induce γ -tubulin organization into native or ectopic MTOCs. Among proteins associated with the centrosome, pericentrin may also be essential for centrosome function (Doxsey et al., 1994). Pericentrin and γ -tubulin form a large soluble complex, which forms a lattice and nucleate microtubules when assembled at the centrosome (Dichtenberg et al., 1998). It is not clear how the γ -tubulin-pericentrin complex assembles or how it is directed to the centrosome. The association

of mNudE with both pericentrin and γ -tubulin makes it an appealing candidate for mediating pericentrin- γ -tubulin complex assembly and centrosomal recruitment. Moreover, centrosomes become heavily phosphorylated as the cell enters mitosis (Kubiak et al., 1992), correlating temporally with a sudden increase in the microtubule-nucleating potential of the centrosome. Since the *Xenopus* mNudE homolog, MP43, is hyperphosphorylated by mitotic cell extracts in vitro (Stukenberg et al., 1997), and since mNudE contains consensus substrate sites for mitosis specific kinases (Figure 1C), mitotic-specific phosphorylation of mNudE/MP43 may be a critical mechanism for regulating centrosomal function. However, this possibility remains to be experimentally tested.

The centrosomal association of LIS1/mNudE further elucidates roles of LIS1 in the formation and orientation of mitotic spindles during cell division. Although LIS1 was initially identified due to its neuronal migration phenotype in humans with heterozygous mutations (Reiner et al., 1993), there is increasing evidence that the non-mammalian homologs of LIS1 function during cell division. The yeast LIS1 homolog, PAC1, is functionally involved in mitotic spindle pole separation (Geiser et al., 1997), and the *Drosophila* LIS1 homolog is essential for germline cell division (Liu, et al., 1999). Moreover, homozygous *Lis1* knockout mice show early postimplantation embryonic lethality, while compound heterozygous *Lis1* mutant mice (which express less than 50% of the wild-type protein level) show defects in the generation as well as in the migration of cerebral cortical neurons (Hirotsume et al., 1998). In *Xenopus* embryos in which LIS1-mNudE/MP43 interactions have been blocked by mNudE-DN injections, we observed abnormalities in the organization of proliferative regions, as well as in regions containing postmitotic neurons (Figure 4), so that roles of mNudE/LIS1 in proliferating neural precursors as well as postmitotic neurons are possible.

The Role of LIS1-mNudE Interactions in CNS Development

The truncated mNudE construct that we overexpressed in *Xenopus* would be expected to block endogenous LIS1 interactions with MP43 and with any other NUDE homologs in *Xenopus*. In mice, there appear to be two proteins with significant homology to NUDE in the coiled-coil LIS1-interacting domain, and both these proteins bind LIS1 (Sasaki et al., 2000; Niethammer et al., 2000). Our dominant-negative construct would have the advantage of blocking LIS1 binding to any *Xenopus* homologs of this family, while presumably allowing interactions of LIS1 or mNudE/MP43 with other proteins to occur.

Both LIS1 and mNudE are ubiquitously expressed, yet only central nervous system (CNS) phenotypes were observed in human heterozygous LIS1 mutations and in our dominant-negative experiments with *Xenopus* embryos. This may reflect a dosage effect in LIS1 function, in which the CNS is more sensitive and is preferentially affected. It seems that further reduction of LIS1 protein levels, as observed with homozygous or compound heterozygous mouse mutations and in *Drosophila* mutants (Hirotsume et al., 1998; Liu et al., 1999; Swan

et al., 1999) are required to bring out the non-CNS phenotypes of LIS1 mutations. Although the widespread expression of both LIS1 and mNudE, and the early lethality of homozygous LIS1 mutations, seem to reflect ubiquitous roles for LIS1-mNudE interactions, the mechanism of the dosage sensitive CNS phenotypes is not yet clear.

The LIS1-mNudE Interaction Is Evolutionarily Conserved
Like *LIS1*, *mNudE* is highly conserved throughout evolution, with high primary sequence conservation particularly in the amino-terminal coiled-coil regions (Figure 1A). This region contains the LIS1 binding domain, it is also necessary and sufficient for NUDE-NUDF interaction and the function of NUDE in *Aspergillus* (Efimov and Morris, 2000). This conservation of protein structure is paralleled by an apparent conservation of protein interactions and functions. In fungus, *NUDF* and *NUDE* share similar nuclear migration phenotypes to mutations in α -, β -, γ -tubulins (*TubA*, *TubB*, *MipA*), as well as the heavy chain (*NUDA*) and the 8 kDa light chain (*NUDG*) of cytoplasmic dynein (Morris et al., 1979; Oakley and Oakley, 1989; Xiang et al., 1994, 1999; Willins et al., 1995). In mammals, we showed that mNudE associates with γ -tubulin and the 8 kDa dynein light chain and LIS1, which also interacts with microtubules and cytoplasmic dynein (Sapir et al., 1997; Smith et al., 2000; Faulkner et al., 2000). These conserved proteins and conserved interactions indicate that the microtubule-based molecular machinery underlying nuclear migration is conserved in fungi and migrating neurons.

Potential Functions of LIS1 and MTOCs in Neuronal Migration

Since *NUDF*'s and *NUDE*'s specific roles in the filamentous fungus relate to nuclear movement, LIS1 and mNudE's role in neuronal migration may reflect an analogous function. Using time-lapse video microscopy, Rakic and others showed that neuronal migration starts with an extension of the leading process of the cell, which is followed by the translocation of the nucleus and the cytoplasmic content (Komuro and Rakic, 1995; Rakic et al., 1996; Hatten, 1999). Moreover, migrating nuclei often associate tightly with MTOCs (reviewed by Reinsch and Gonczy, 1998). Similar links between MTOC and direction of cell movement have been observed in other cell types. In migrating *Dictyostelium*, cells often extend two to three pseudopodia in different directions in rapid succession. Centrosomes labeled by GFP- γ -tubulin would eventually follow one pseudopod, while pseudopodia into which the centrosome did not reorient were retracted quickly. Therefore, microtubules may help to establish and maintain the direction of cell migration, while the centrosome acts as a stabilizer of cell migration (Ueda et al., 1997, 1999). By controlling the formation of a functional centrosome, LIS1-mNudE interactions may be crucial for maintaining the dynamic stability of microtubules in migrating neurons. Our data suggest a tentative model on the mechanism LIS1-mNudE based nuclear migration in migrating cortical neurons (Figure 8). In this model, we hypothesize that a regulated LIS1-mNudE interaction at the centrosome results in microtubule shortening in the leading process

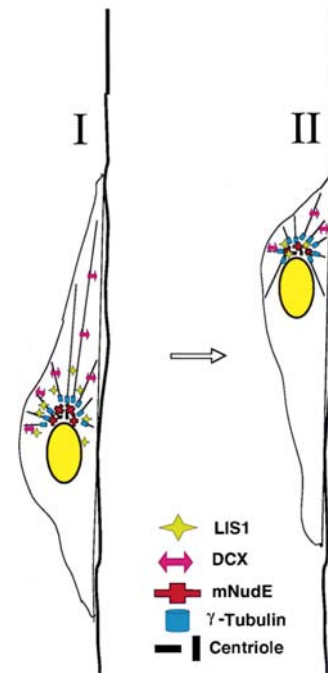


Figure 8. Schematic Model of How LIS1 and mNudE Might Regulate Nuclear Migration in a Migrating Neuron

Neuronal migration along the radial glia starts with the extension of the leading process, which is followed by the translocation of the nucleus and the cytoplasmic content; migrating nuclei often associate tightly with the centrosome. Combining these previous observations and our experimental data suggests the following model. From stage I to stage II, microtubule-based migration may be dissected into several steps. First, cells receive migration signals and microtubules extend in the leading process. This may be regulated by DCX and other MAPs. Second, a regulatory event leads the recruitment of LIS1 to MTOC through binding to mNudE. The regulation of LIS1 may be mediated by phosphorylation or other modifications. Third, interaction of LIS1 with mNudE at the centrosome reduces the nucleation and polymerization of microtubules at the minus end, possibly by regulating the γ -tubulin complex. Finally, as a result, microtubules shorten at the minus end and the nucleus is pulled toward the leading edge of the migrating neuron. Microtubules in the leading end of the cell are depicted as dark thin lines. Microtubules at the trailing end of the cell are not illustrated. The membrane of the radial glial fiber to which the migrating neuron is attached is depicted by a thick dark line.

of the migrating neurons and translocation of the nucleus. However, future studies on how the LIS1-mNudE interaction is regulated at the centrosome and how microtubule shortening is achieved are essential to test this hypothesis.

LIS1 and Other Lissencephaly Genes in Neuronal Migration

The phenotype of heterozygous *LIS1* mutations in humans strongly resembles the phenotype of mutations in the X-linked *DCX* gene (Berg et al., 1998; Dobyns et al., 1999). *DCX* also encodes a microtubule-associated protein that has been shown to be a potent microtubule stabilizer (Francis et al., 1999; Gleeson et al., 1999). However, *DCX* does not appear to act through *mNudE*, since *DCX* shows a widespread subcellular distribution and a very tight, apparently direct, association with α

and β tubulin. Thus, LIS1 and DCX seem to focus upon the stabilization of microtubules but may act upon different microtubule components.

Mutations of Cdk5 and P35 in mouse were also shown to cause neuronal migration defects (Ohshima et al., 1996; Chae et al., 1997). Moreover, the Cdk5/P35 complex may regulate microtubule structure by phosphorylating tau under normal and pathological conditions (Patrick et al., 1999). mNudE contains potential phosphorylation sites for Cdk5 and many other kinases (Figure 1C). In fact, phosphorylation of NUDEL, a close homolog of mNudE, by Cdk5 has recently been shown (Sasaki et al., 2000; Niethammer et al., 2000). Thus, mNudE and NUDEL might represent points of convergence for upstream migration signals to regulate microtubule structures. It would be of great interest to further investigate how mNudE's function is regulated by other lissencephaly or neuronal migration genes. The continued genetic analysis of neuronal migration disorders in humans and mice promises a continued dissection of cytoskeletal elements that are crucial to neuronal function.

Experimental Procedures

Yeast Two-Hybrid Screen

The yeast two-hybrid screen was performed as previously described (Vojtek et al., 1993), using full-length human LIS1 cDNA fused in frame to LexA (LexA-LIS1) as the bait. A L40 yeast strain was transformed with LexA-LIS1, then transformed with a mouse E10.5 total embryonic cDNA library (a gift from Dr. Stan Hollenberg). An estimated 5×10^6 transformants were plated for histidine selection, and about 700 transformants were recovered after 3–5 days at 30°C. The mNudE two-hybrid screen used full-length mNudE as the bait, and 42 positive clones were recovered out of estimated 1×10^6 total transformants. Histidine-positive colonies were collected and screened for β -galactosidase activity using a filter assay (Breedon and Nasmyth, 1985) and were confirmed as "true positive" clones by plasmid isolation (Hoffman and Winston, 1987) and retransformation into bait containing L40 stain.

mNudE cDNA Cloning

The full-length mNudE cDNA sequence was obtained by (1) screening a λ -ZAP II mouse P0 brain cDNA library (Stratagene), (2) 5' and 3' RACE PCR from mouse E16 Marathon-ready cDNAs library (Clontech), and (3) analysis of the mouse EST database. A full-length mNudE cDNA clone was obtained by cloning the RT-PCR product from mouse E16 brain mRNA. DNA sequencing was performed by the DyeDeoxy terminator cycle sequencing kit protocol (Applied Biosystems).

Plasmid Construction

Cloning and subcloning strategies used for making plasmids described in this study are available upon request (yfeng@caregroup.harvard.edu) but are omitted to save space. LexA-LIS1 was made by cloning full-length LIS1 cDNA into pBTM116. LIS1 was myc tagged at the amino terminus and subcloned into pcDNA3 (Invitrogen) to form myc-LIS1. LIS1H149R and LIS1S169P were made using the Stratagene Quickchange site-directed mutagenesis system with the standard protocol provided by the manufacturer using LexA-LIS1 and myc-LIS1 as templates. Full-length mNudE was myc-tagged at the amino terminus and cloned into the pcDNA3 to obtain myc-mNudE. GFP-mNudE was constructed by replacing the tubulin coding region with mNudE cDNA in EGFP-Tubulin plasmid (Clontech). mNudE-EGFP was made by inserting mNudE into pEGFP-1 (Clontech), then further subcloned into pcDNA3. To construct GFP-LIS1, the LIS1 coding sequences was used to replace the mNudE coding sequence in GFP-mNudE-pcDNA3. GST-mNudE was made by inserting myc-mNudE into the GST2T vector (Pharmacia). LexA-mNudE was made by cloning mNudE into pBTM116. VP16-mNudE

was made by cloning mNudE cDNA into a modified pVP16 vector at a newly created EcoR I site. CS2+myc-mNudE was constructed by removing myc-mNudE from pcDNA3 and religating into CS2+ vector (Turner and Weintraub, 1994). CS2+DN was constructed by PCR amplification of the region encoding amino acids 88–156 of the mNudE cDNA and subcloning into the CS2+ vector. The same fragment was used to create GFP-DN in pcDNA3. All PCR products used in this study were sequenced to confirm that no undesired mutation occurred during in vitro DNA synthesis.

Antibodies

A synthetic peptide corresponding to amino acid 1–13 of the mNudE sequence was coupled to KLH and injected into rabbits for producing antisera. The resulting antisera were used directly by diluting at 1:600 for immunostaining and 1:2000 for immunoblotting. Alternatively, the antisera were purified using a peptide affinity column (Affi-Gel 10 Gel, Bio-Rad) according to the manufacturer's instruction.

Monoclonal anti human c-myc antibody 9E10 and polyclonal anti-LIS1 antibody N-19 were from Santa Cruz. Monoclonal anti- γ -tubulin antibody GTU-88 and monoclonal anti- α -tubulin B-5-1-2 antibody were from Sigma. Monoclonal and polyclonal anti-GFP antibodies were from Clontech. A mouse monoclonal anti-LIS1 antibody was a gift from Dr. O. Reiner. Polyclonal anti LIS1 antisera N1 was a gift from Dr. M. Mizuguchi.

RNA Analyses

For Northern blotting, total RNA was extracted from mouse tissues using Ultraspec RNA reagents (Biotecx, Houston, Texas). Total RNA (5 or 10 μ g) was electrophoresed and transferred to a nylon filter using standard techniques. DNA probes were radiolabeled with α - 32 P dCTP using the Megaprime DNA labeling system (Amersham). Hybridization was performed in ExpressHyb solution (Clontech) according to the manufacturer's protocol. Mouse G3PDH cDNA and β -actin probes were used to normalize loading. In situ hybridization of mouse embryos was performed essentially as described (Wilkinson and Nieto, 1993). Sections were developed with NBT/BCIP (Boehringer Mannheim) with polyvinyl alcohol and Levamisole at 37°C. Whole-mount in situ hybridization of *Xenopus* Albino embryos was performed as described (Harland, 1991) using a (DIG)-labeled antisense MP43 RNA probe.

RNA Expression in *Xenopus*

GFP-CS2+, mNudE-DN-CS2+, and myc-mNudE-CS2+ were linearized. Capped RNA were produced in vitro using the Mega prime RNA Kit (Ambion), performed according to manufacturer's instructions, and supplemented with 6 mM m^7 G(5')ppp(5') G and 1.5 mM GTP. Embryos were injected with 1–3 ng of RNA into the right blastomere at the two-cell or four-cell stage in $0.1 \times$ MMR (100 mM NaCl, 2 mM KCl, 1 mM $MgCl_2$, 2 mM $CaCl_2$), supplemented with 6% Ficoll, and transferred to $0.1 \times$ MMR after gastrulation.

Histological Analysis

Xenopus embryos were fixed in MEMFA (0.1M MOPS [pH 7.4], 2 mM EGTA, 1 mM $MgSO_4$, 3.7% formaldehyde) for 2 hr at room temperature and then dehydrated in methanol and stored at -20° C. Paraffin embedding and sectioning were performed with standard protocol. The sections were stained with haematoxylin and eosin (H&E) according to standard procedure.

Cell Culture and Transfection

COS-7 cells and 293T cells were grown in DMEM supplemented with 10% FBS. Mouse E16 cortical primary neurons were isolated and cultured on poly-D-lysine coated cover slips according to Ghosh and Greenberg (1995). Transient transfection was done using Lipofectamine Reagent (GIBCO-BRL) according to the manufacturer's instructions. Cells were harvested 28–44 hr after transfection.

Immunohistochemistry and Indirect

Immunofluorescence Microscopy

E16 mouse brain was embedded in OCT, sectioned at 20 μ m, and fixed in methanol at -20° C. Sections were rehydrated stepwise in 95%, 75%, 50% ethanol and PBS and stained with mNudE antisera

and Cy3-conjugated goat anti-rabbit antibody (Jackson ImmunoResearch Labs) using standard procedure.

Cells grown on cover slips were rinsed once with PBS, then fixed in either -20°C methanol or 4% methanol-free formaldehyde (Ted Pella) in a staining buffer containing 25 mM HEPES (pH 7.4), 250 mM Sucrose, 2.5 mM KCl, and 2.5 mM MgAc_2 for 10 min. Following fixation, the rest of the staining was all performed in the staining buffer as described (Campbell et al., 1992).

Protein Extraction and Immunoprecipitation

Cells grown as monolayers on tissue culture dishes were washed two times with PBS and collected in PBS containing 1 mM EDTA. After two subsequent washes in PBS by low-speed centrifugation, cell pellets were resuspended in lysis buffer I (100 mM NaCl, 50 mM Tris-HCl [pH 7.4], 2 mM EDTA, 10 mM NaF, 10% Glycerol, 0.1% Triton X-100, and 1 mM DTT) or lysis buffer II (100 mM NaCl, 20 mM HEPES [pH 7.4], 1 mM EDTA, 10 mM MgCl_2 , 0.02% Triton X-100, and 1 mM DTT) in the presence of 10 mM Na_3VO_4 and protease inhibitors (10 $\mu\text{g}/\text{ml}$ Leupeptin, 10 $\mu\text{g}/\text{ml}$ Pepstatin A, 50 mM Benzamide, and 2 mM PMSF). After cell lysis is complete, lysates were cleared by spinning in a microcentrifuge at 14,000 rpm for 15 min, and supernatants were removed and used for immunoblotting or immunoprecipitation analyses. Immunoprecipitations were performed with about 500 μg protein extracts and 1–2 μg purified monoclonal antibodies. The immunoreaction mixtures were incubated for 2 hr on ice and spun at 14,000 rpm for 15 min. The supernatants were further incubated with 15 μl of protein A-sepharose CL-4B (Pharmacia) at 4°C on a rotator for 1 hr. The protein A-sepharose beads were brought down by low-speed centrifugation and washed six times with binding buffer. The proteins that precipitate with the protein A-sepharose were eluted with $1\times$ SDS-PAGE sample buffer and analyzed by SDS-PAGE followed by immunoblotting.

To detect native mNudE on immunoblot, mouse embryonic tissues were homogenized in 250 mM sucrose, 10 mM Tris [pH 7.5], 10 mM MgCl_2 , supplemented with protease and phosphates inhibitors as in extraction buffers I and II. The homogenate was spun down in a microcentrifuge at 14,000 rpm. The supernatant was used for immunoblotting.

Acknowledgments

We would like to thank S. Hollenberg, Q. Lu, and C. Weitz for providing two-hybrid libraries, D. Chang and D. Turner for providing constructs, and O. Reiner and M. Mizuguchi for kindly supplying LIS1 antibodies. We thank P. Dikkes and S. Rankin for help in histological analysis of *Xenopus* embryos and M. Zuber and K. Kroll for helpful discussions and suggestions on *Xenopus* analyses and data interpreting. We thank V. Efimov, N. R. Morris, S. Hirotsune, A. Wynshaw-Boris, and L.-H. Tsai for communicating their unpublished results. We thank L. Evans for help with the *Xenopus* whole-mount in situ hybridization. We also thank T. Chae, A. Chenn, J. Corbo, J. Gleeson, P. Lin, G. Mochida, E. Monuki, M. Neito, V. Sheen, and other members of the Walsh lab for helpful comments and stimulating discussions. This work was supported by grants from NINDS to C. A. W. (P01-NS 39404 and P01-NS 40043), by a NRSA postdoctoral fellowship to Y. F. (F32-NS 10730), and by the Mental Retardation Research Center at the Children's Hospital, Boston.

Received October 12, 2000; revised November 22, 2000.

References

Alvarez, L.A., Yamamoto, T., Wong, B., Resnick, T.J., Llana, J.F., and Moshe, S.L. (1986). Miller-Dieker syndrome: a disorder affecting specific pathways of neuronal migration. *Neurology* 36, 489–493.

Berg, M.J., Schifitto, G., Powers, J.M., Martinez-Capolino, C., Fong, C.T., Myers, G.J., Epstein, L.G., and Walsh, C.A. (1998). X-linked female band heterotopia-male lissencephaly syndrome. *Neurology* 50, 1143–1146.

Breeden, L., and Nasmyth, K. (1985). Regulation of the yeast HO gene. *Cold Spring Harb. Symp. Quant. Biol.* 50, 643–650.

Brown, C.R., Doxsey, S.J., Hong-Brown, L.Q., Martin, R.L., and Welch, W.J. (1996). Molecular chaperones and the centrosome. A

role for TCP-1 in microtubule nucleation. *J. Biol. Chem.* 271, 824–832.

Chae, T., Kwon, Y.T., Bronson, R., Dikkes, P., Li, E., and Tsai, L.H. (1997). Mice lacking p35, a neuronal specific activator of Cdk5, display cortical lamination defects, seizures, and adult lethality. *Neuron* 18, 29–42.

Campbell, A.M., Kessler, P.D., and Fambrough, D.M. (1992). The alternative carboxyl termini of avian cardiac and brain sarcoplasmic reticulum/endoplasmic reticulum $\text{Ca}(2+)$ -ATPases are on opposite sides of the membrane. *J. Biol. Chem.* 267, 9321–9325.

Dick, T., Ray, K., Salz, H.K., and Chia, W. (1996). Cytoplasmic dynein (ddlc1) mutations cause morphogenetic defects and apoptotic cell death in *Drosophila melanogaster*. *Mol. Cell Biol.* 16, 1966–1977.

Dictenberg, J.B., Zimmerman, W., Sparks, C.A., Young, A., Vidair, C., Zheng, Y., Carrington, W., Fay, F.S., and Doxsey, S.J. (1998). Pericentrin and gamma-tubulin form a protein complex and are organized into a novel lattice at the centrosome. *J. Cell Biol.* 141, 163–174.

Dobyns, W.B., Truwit, C.L., Ross, M.E., Matsumoto, N., Pilz, D.T., Ledbetter, D.H., Gleeson, J.G., Walsh, C.A., and Barkovich, A.J. (1999). Differences in the gyral pattern distinguish chromosome 17-linked and X-linked lissencephaly. *Neurology* 53, 270–277.

Doxsey, S.J., Stein, P., Evans, L., Calarco, P.D., and Kirschner, M. (1994). Pericentrin, a highly conserved centrosome protein involved in microtubule. *Cell* 76, 639–650.

Efimov, V.P., and Morris, N.R. (2000). The LIS1-related NUDF Protein of *Aspergillus nidulans* Interacts with the Coiled Coil Domain of the NUDE/RO11 Protein. *J. Cell Biol.*, in press.

Faulkner, N.E., Dujardin, D.L., Tai, C., Vaughan, K.T., O'Connell, C.B., Wang, Y., and Vallee, R.B. (2000). A role for the lissencephaly gene LIS1 in mitosis and cytoplasmic dynein function. *Nat Cell Biol.* 2, 784–791.

Francis, F., Koulakoff, A., Boucher, D., Chafey, P., Schaar, B., Vinet, M.C., Friocourt, G., McDonnell, N., Reiner, O., Kahn, A., et al. (1999). Doublecortin is a developmentally regulated, microtubule-associated protein expressed in migrating and differentiating neurons. *Neuron* 23, 247–256.

Geiser, J.R., Schott, E.J., Kingsbury, T.J., Cole, N.B., Totis, L.J., Bhattacharyya, G., He, L., and Hoyt, M.A. (1997). *Saccharomyces cerevisiae* genes required in the absence of the CIN8-encoded spindle motor act in functionally diverse mitotic pathways. *Mol. Biol. Cell* 8, 1035–1050.

Ghosh, A., and Greenberg, M.E. (1995). Distinct roles for bFGF and NT-3 in the regulation of cortical neurogenesis. *Neuron* 15, 89–103.

Gleeson, J.G., and Walsh, C.A. (2000). Neuronal migration disorders: from genetic disease to developmental mechanisms. *Trends Neurosci.* 23, 352–359.

Gleeson, J.G., Allen, K.M., Fox, J.W., Lamperti, E.D., Berkovic, S., Scheffer, I., Cooper, E.C., Dobyns, W.B., Minnerath, S.R., Ross, M.E., and Walsh, C.A. (1998). Doublecortin, a brain-specific gene mutated in human X-linked lissencephaly and double cortex syndrome, encodes a putative signaling protein. *Cell* 92, 63–72.

Gleeson, J.G., Lin, P.T., Flanagan, L.A., and Walsh, C.A. (1999). Doublecortin is a microtubule-associated protein and is expressed widely by migrating neurons. *Neuron* 23, 257–271.

Guasch, G., Mack, G.J., Popovici, C., Dastugue, N., Birnbaum, D., Rattner, J.B., and Pebusque, M.J. (2000). FGFR1 is fused to the centrosome-associated protein CEP110 in the 8p12 stem cell myeloproliferative disorder with t(8;9)(p12;q33). *Blood* 95, 1788–1796.

Guzzo, R.M., Salih, M., Wielowieyski, P., Wigle, J.T., and Tuana, B.S. (1999). Targeting of sarcolemmal associated proteins (SLAPs) to cellular membranes and the microtubule organizing center (MTOC). *Mol. Biol. Cell* 10, 16a.

Hatten, M.E. (1999). Central nervous system neuronal migration. *Annu. Rev. Neurosci.* 22, 511–539.

Harland, R.M. (1991). In situ hybridization: an improved whole mount method for *Xenopus* embryos. *Methods Cell Biol.* 36, 685–695.

Hirotsune, S., Fleck, M.W., Gambello, M.J., Bix, G.J., Chen, A., Clark, G.D., Ledbetter, D.H., McBain, C.J., and Wynshaw-Boris, A. (1998).

- Graded reduction of Pafah1b1 (Lis1) activity results in neuronal migration defects and early embryonic lethality. *Nat. Genet.* 19, 333–339.
- Hoffman, C.S., and Winston, F. (1987). A ten-minute DNA preparation from yeast efficiently releases autonomous plasmids for transformation of *Escherichia coli*. *Gene* 57, 267–272.
- Jellinger, K., and Rett, A. (1976). Agyria-pachygyria (lissencephaly syndrome). *Neuropadiatrie* 7, 66–91.
- Kitagawa, M., Umezumi, M., Aoki, J., Koizumi, H., Arai, H., and Inoue, K. (2000). Direct association of LIS1, the lissencephaly gene product, with a mammalian homologue of a fungal nuclear distribution protein, rNUDE. *FEBS Lett.* 479, 57–62.
- Komuro, H., and Rakic, P. (1995). Dynamics of granule cell migration: a confocal microscopic study in acute cerebellar slice preparations. *J. Neurosci.* 15, 1110–1120.
- Kuchelmeister, K., Bergmann, M., and Gullotta, F. (1993). Neuropathology of lissencephalies. *Childs Nerv Syst* 9, 394–399.
- Kubiak, J.Z., Weber, M., Geraud, G., and Maro, B. (1992). Cell cycle modification during the transitions between meiotic M-phases in mouse oocytes. *J. Cell Sci.* 102, 457–467.
- Li, Q., Ke, Y., Kapp, J.A., Fertig, N., Medsger, T.A., Jr., and Joshi, H.C. (1995). A novel cell-cycle-dependent 350-kDa nuclear protein: C-terminal domain sufficient for nuclear localization. *Biochem. Biophys. Res. Commun.* 212, 220–228.
- Liu, Z., Xie, T., and Steward, R. (1999). Lis1, the *Drosophila* homolog of a human lissencephaly disease gene, is required for germline cell division and oocyte differentiation. *Development* 126, 4477–4488.
- Lo Nigro, C., Chong, C.S., Smith, A.C., Dobyns, W.B., Carrozzo, R., and Ledbetter, D.H. (1997). Point mutations and an intragenic deletion in LIS1, the lissencephaly causative gene in isolated lissencephaly sequence and Miller-Dieker syndrome. *Hum. Mol. Genet.* 6, 157–164.
- Lupas, A., Van Dyke, M., Stock, J. (1991). Predicting coiled coils from protein sequences. *Science* 252, 1162–1164.
- Minke, P.F., Lee, I.H., Tinsley, J.H., Bruno, K.S., and Plamann, M. (1999). *Neurospora crassa* ro-10 and ro-11 genes encode novel proteins required for nuclear distribution. *Mol. Microbiol.* 32, 1065–1076.
- Morris, N.R., Lai, M.H., and Oakley, C.E. (1979). Identification of a gene for alpha-tubulin in *Aspergillus nidulans*. *Cell* 16, 437–442.
- Morris, S.M., Albrecht, U., Reiner, O., Eichele, G., and Yu-Lee, L.Y. (1998a). The lissencephaly gene product Lis1, a protein involved in neuronal migration, interacts with a nuclear movement protein, NudC. *Curr. Biol.* 8, 603–606.
- Morris, N.R., Efimov, V.P., and Xiang, X. (1998b). Nuclear migration, nucleokinesis and lissencephaly. *Trends Cell Biol.* 8, 467–470.
- Niethammer, M., Smith, D.S., Ayala, R., Peng, J., Ko, J., Lee, M.-S., Morabito, M., and Tsai, L.-H. (2000). NUDEL is a novel Cdk5 substrate that associates with LIS1 and cytoplasmic dynein. *Neuron* 28, this issue, 697–711.
- Oakley, C.E., and Oakley, B.R. (1989). Identification of gamma-tubulin, a new member of the tubulin superfamily encoded by mipA gene of *Aspergillus nidulans*. *Nature* 338, 662–664.
- Ohshima, T., Ward, J.M., Huh, C.G., Longenecker, G., Veeranna, Pant, H.C., Brady, R.O., Martin, L.J., and Kulkarni, A.B. (1996). Targeted disruption of the cyclin-dependent kinase 5 gene results in abnormal corticogenesis, neuronal pathology and perinatal death. *Proc. Natl. Acad. Sci. USA* 93, 11173–11178.
- Patrick, G.N., Zukerberg, L., Nikolic, M., de la Monte, S., Dikkes, P., and Tsai, L.H. (1999). Conversion of p35 to p25 deregulates Cdk5 activity and promotes neurodegeneration. *Nature* 402, 615–622.
- Pilz, D.T., Kuc, J., Matsumoto, N., Bodurtha, J., Bernadi, B., Tassinari, C.A., Dobyns, W.B., and Ledbetter, D.H. (1999). Subcortical band heterotopia in rare affected males can be caused by missense mutations in DCX (XLIS) or LIS1. *Hum. Genet.* 8, 1757–1760.
- Purohit, A., Tynan, S.H., Vallee, R., and Doxsey, S.J. (1999). Direct interaction of pericentrin with cytoplasmic dynein light intermediate chain contributes to mitotic spindle organization. *J. Cell Biol.* 147, 481–492.
- Rakic, P. (1978). Neuronal migration and contact guidance in the primate telencephalon. *Postgrad Med J* 54, 25–40.
- Rakic, P., Knyihar-Csillik, E., and Csillik, B. (1996). Polarity of microtubule assemblies during neuronal cell migration. *Proc. Natl. Acad. Sci. USA* 93, 9218–9222.
- Rattner, J.B., Rao, A., Fritzler, M.J., Valencia, D.W., and Yen, T.J. (1993). CENP-F is a 400 kDa kinetochore protein that exhibits a cell-cycle dependent localization. *Cell Motil Cytoskeleton* 26, 214–226.
- Reiner, O., Carrozzo, R., Shen, Y., Wehnert, M., Faustinella, F., Dobyns, W.B., Caskey, C.T., and Ledbetter, D.H. (1993). Isolation of a Miller-Dieker lissencephaly gene containing G protein beta-subunit-like repeats. *Nature* 364, 717–721.
- Reinsch, S., and Gonczy, P. (1998). Mechanism of nuclear positioning. *J. Cell Sci.* 111, 2283–2295.
- Sapir, T., Elbaum, M., and Reiner, O. (1997). Reduction of microtubule catastrophe events by LIS1, platelet-activating factor acetylhydrolase subunit. *EMBO J.* 16, 6977–6984.
- Sapir, T., Cahana, A., Seger, R., Nekhai, S., and Reiner, O. (1999a). LIS1 is a microtubule-associated phosphoprotein. *Eur. J. Biochem.* 265, 181–188.
- Sapir, T., Eisenstein, M., Burgess, H.A., Horesh, D., Cahana, A., Aoki, J., Hattori, M., Arai, H., Inoue, K., and Reiner, O. (1999b). Analysis of lissencephaly-causing LIS1 mutations. *Eur. J. Biochem.* 266, 1011–1020.
- Sasaki, S., Shionoya, A., Ishida, M., Gambello, M.J., Yingling, J., Wynshaw-Boris, A., and Hirotsune, S. (2000). A LIS1/NUDEL/cytoplasmic dynein heavy chain complex in the developing and adult nervous system. *Neuron* 28, this issue, 681–696.
- Shu, H.B., and Joshi, H.C. (1995). Gamma-tubulin can both nucleate microtubule assembly and self-assemble into novel tubular structures in mammalian cells. *J. Cell Biol.* 130, 1137–1147.
- Smith, D.S., Niethammer, M., Ayala, R., Zhou, Y., Gambello, M.J., Wynshaw-Boris, A., and Tsai, L. (2000). Regulation of cytoplasmic dynein behaviour and microtubule organization by mammalian Lis1. *Nat. Cell Biol.* 2, 767–775.
- Songyang, Z., and Cantley, L.C. (1998). The use of peptide library for the determination of kinase peptide substrates. *Methods Mol. Biol.* 87, 87–98.
- Stearns, T., Evans, L., and Kirschner, M. (1991). Gamma-tubulin is a highly conserved component of the centrosome. *Cell* 65, 825–836.
- Stearns, T., and Kirschner, M. (1994). In vitro reconstitution of centrosome assembly and function: the central role of gamma-tubulin. *Cell* 76, 623–637.
- Stukenberg, P.T., Lustig, K.D., McGarry, T.J., King, R.W., Kuang, J., and Kirschner, M.W. (1997). Systematic identification of mitotic phosphoproteins. *Curr. Biol.* 7, 338–348.
- Swan, A., Nguyen, T., and Suter, B. (1999). *Drosophila* Lissencephaly-1 functions with Bic-D and dynein in oocyte determination and nuclear positioning. *Nat. Cell Biol.* 1, 444–449.
- Turner, D.L., and Weintraub, H. (1994). Expression of achaete-scute homolog 3 in *Xenopus* embryos converts ectodermal cells to a neural fate. *Genes Dev.* 8, 1434–1447.
- Ueda, M., Graf, R., MacWilliams, H.K., Schliwa, M., and Euteneuer, U. (1997). Centrosome positioning and directionality of cell movements. *Proc. Natl. Acad. Sci. USA* 94, 9674–9678.
- Ueda, M., Schliwa, M., and Euteneuer, U. (1999). Unusual centrosome cycle in *Dictyostelium*: correlation of dynamic behavior and structural changes. *Mol. Biol. Cell* 10, 151–160.
- Vojtek, A.B., Hollenberg, S.M., and Cooper, J.A. (1993). Mammalian Ras interacts directly with the serine/threonine kinase Raf. *Cell* 74, 205–214.
- Walsh, C.A. (1999). Genetic malformations of the human cerebral cortex. *Neuron* 23, 19–29.
- Willins, D.A., Xiang, X., and Morris, N.R. (1995). An alpha tubulin mutation suppresses nuclear migration mutations in *Aspergillus nidulans*. *Genetics* 141, 1287–1298.
- Wilkinson, D.G., and Nieto, M.A. (1993). Detection of messenger RNA

by in situ hybridization to tissue sections and whole mounts. *Methods Enzymol.* 225, 361–373.

Xiang, X., Beckwith, S.M., and Morris, N.R. (1994). Cytoplasmic dynein is involved in nuclear migration in *Aspergillus nidulans*. *Proc. Natl. Acad. Sci. USA* 91, 2100–2104.

Xiang, X., Osmani, A.H., Osmani, S.A., Xin, M., and Morris, N.R. (1995). NudF, a nuclear migration gene in *Aspergillus nidulans*, is similar to the human LIS-1 gene required for neuronal migration. *Mol. Biol. Cell* 6, 297–310.

Xiang, X., Zuo, W., Efimov, V.P., and Morris, N.R. (1999). Isolation of a new set of *Aspergillus nidulans* mutants defective in nuclear migration. *Curr. Genet.* 35, 626–630.

Zheng, Y., Wong, M.L., Alberts, B., and Mitchison, T. (1995). Nucleation of microtubule assembly by a gamma-tubulin-containing ring complex. *Nature* 378, 578–583.

GenBank Accession Number

The accession number for the mNudE sequence is AF322073.